SPECTROSCOPIC METHODOLOGY – Notes

Magnetic Resonance in Medicine 72:934–940 (2014)

Is the Macromolecule Signal Tissue-Specific in Healthy Human Brain? A ^{1}H MRS Study at 7 Tesla in the Occipital Lobe

Benoît Schaller,[1] Lijing Xin,[2] and Rolf Gruetter[1,2,3]

Purpose: The macromolecule signal plays a key role in the precision and the accuracy of the metabolite quantification in short-TE ^{1}H MR spectroscopy. Macromolecules have been reported at 1.5 Tesla (T) to depend on the cerebral studied region and to be age specific. As metabolite concentrations vary locally, information about the profile of the macromolecule signal in different tissues may be of crucial importance.

Methods: The aim of this study was to investigate, at 7T for healthy subjects, the neurochemical profile differences provided by macromolecule signal measured in two different tissues in the occipital lobe, predominantly composed of white matter tissue or of grey matter tissue.

Results: White matter-rich macromolecule signal was relatively lower than the gray matter-rich macromolecule signal from 1.5 to 1.8 ppm and from 2.3 to 2.5 ppm with mean difference over these regions of 7% and 12% (relative to the reference peak at 0.9 ppm), respectively. The neurochemical profiles, when using either of the two macromolecule signals, were similar for 11 reliably quantified metabolites (CRLB $< 20\%$) with relatively small concentration differences (< 0.3 μmol/g), except Glu (± 0.8 μmol/g).

Conclusion: Given the small quantification differences, we conclude that a general macromolecule baseline provides a sufficiently accurate neurochemical profile in occipital lobe at 7T in healthy human brain. **Magn Reson Med 72:934–940, 2014.**

Key words: In vivo ^{1}H MRS; macromolecule signal; metabolite quantification; neurochemical profile; 7T; healthy human brain

INTRODUCTION

Signal-to-noise ratio (SNR) and chemical shift dispersion increase at high magnetic field (≥7 Tesla [T]), allowing improved accuracy and precision of metabolite quantification (1–3). In addition, when using short echo times (TE < 10 ms), signal modulations of J-coupled resonances and T_2-losses are minimized, resulting in a neurochemical profile including a large number of metabolites (4–6). However, a broad underlying signal, e.g., cytosolic proteins, overlaps with metabolite resonances at short TE (7–9). Macromolecule signal has been characterized by short T_1 and T_2 (10,11) and low apparent diffusion coefficients (12). It can potentially affect the accuracy of the quantification even when considering healthy brain tissue (13,14). At low field (≤3T), the mathematical approximation (spline baseline) is a sufficient estimation of the macromolecule contribution to ^{1}H spectra at 3T (15). However, because of the increased spectral resolution at high field (≥7T), distinct macromolecule resonances are observed and the acquisition of the in vivo macromolecule signal is required for an accurate quantification of the neurochemical profile (16–18).

Macromolecule resonances have been reported to be age-specific and to vary with the local brain structure for healthy subjects (19). In addition, Mader et al (20) reported a higher macromolecule concentration in cerebellum and motor cortex than in pons and white matter attributed to a higher relative proportion of grey matter. Finally, a recent study (21) at 3T suggested that the macromolecule signal may vary between healthy subjects, which suggested the need for measurement of the macromolecule signal in each subject. However, the region specificity of the macromolecule signal was reported to be marginal in the rat brain with a minimal impact on the neurochemical profile (22).

As metabolite concentrations have been reported to vary regionally in the human brain (23,24), knowledge about the macromolecule signal in different tissues is of potential interest for an accurate estimation of the metabolite concentration. At low field, the broad spectral pattern of the macromolecules may only affect minimally the metabolite concentration. However, the precise macromolecule profile at high field may influence substantially the metabolite quantification.

Therefore, the aim of the present study was to determine the influence of the macromolecule signal measured in two different tissues in the occipital lobe (grey matter, GM, and white matter, WM) on the neurochemical profile at 7T.

METHODS

Participants

Ten healthy subjects (eight men, two women, ages 20 to 28 years) participated in the study and gave informed consent according to the procedure approved by the

[1]Laboratory of Functional and Metabolic Imaging, Ecole Polytechnique Fédèrale de Lausanne, Lausanne, Switzerland.

[2]Department of Radiology, University Hospitals of Lausanne, Switzerland..

[3]Department of Radiology, University Hospitals of Geneva, Switzerland.

Grant sponsor: SNF; Grant number: 131087.

*Correspondence to: Lijing Xin, Ecole Polytechnique Federale de Lausanne, SB-IPMC-LIFMET, Station 6, 1015 Lausanne, Switzerland. E-mail: lijing.xin@epfl.ch

Received 23 May 2013; revised 23 August 2013; accepted 18 September 2013

DOI 10.1002/mrm.24995

Published online 11 November 2013 in Wiley Online Library (wileyonlinelibrary.com).

local ethics committee. The experiments were performed on a 7T/68 cm scanner (Siemens Healthcare, Erlangen, Germany) with the use of a home-built shielded quadrature transmit/receive surface radiofrequency coil (Ø = 13 cm, circular loops).

Magnetic Resonance Protocol

3D anatomical images were acquired using MP2RAGE (25) (TE/TR = 3.37/5000 ms, TI_1/TI_2 = 700/2200 ms, slice thickness = 1 mm, field of view = 176 × 256 mm^2, matrix size = 176 × 256) and guided the placement of the voxel in the region of interest. Two locations in the occipital lobe were investigated, predominantly composed of grey matter tissue (GM, n = 4) or of white matter tissue (WM, n = 4). A home-written segmentation tool (26) was used to determine the composition of the voxel of interest (VOI) based on signal intensity by segmentation of 3 D images in terms of WM tissue, GM tissue and cerebral spinal fluid. All first- and second-order shim terms were adjusted using FASTMAP (27,28) to optimize B_0 homogeneities over the voxel of interest (GM-rich VOI = 20 × 15 × 20 mm^3 and WM-rich VOI = 15 × 20 × 20 mm^3).

Macromolecule spectra were acquired in the aforementioned locations using the semi-adiabatic Spin Echo full Intensity Acquired Localized (SPECIAL) sequence (TR/TE = 7500/12 ms, vector size = 2048 pts) (10) preceded by an adiabatic full passage inversion pulse (pulse duration = 5.12 ms, bandwidth = 3.9 kHz, $\gamma/2\pi \cdot B_{1max}$ = 1.4 kHz). Before the semi-adiabatic SPECIAL sequence, VAPOR water suppression and outer volume saturation (OVS) (5) were used to minimize the contribution of water and extra-cerebral fat tissue to the spectra. To determine the optimum TI with the smallest metabolite residuals, an initial inversion recovery (IR) experiment was first performed with a set of different inversion times (TI from 800–1000 ms with steps of 50 ms, n = 1). Based on the initial IR experiment, macromolecule spectra were then acquired with the IR semi-adiabatic SPECIAL sequence using a fixed TI (TI = 950 ms, NT = 32 × 2, n = 4 for each region). In addition, macromolecule spectra were acquired for each subject with a TE of 30 ms to identify the metabolite residuals (TI = 950 ms, NT = 16 × 2, n = 4). Finally, ^{1}H spectra were acquired in occipital GM-rich tissue and occipital WM-rich tissue with the standard semi-adiabatic SPECIAL sequence without inversion pulse (NT = 16 × 2, n = 10 for GM-rich ^{1}H spectra and n = 6 for WM-rich ^{1}H spectra).

Data Analysis

After Fourier transformation, the individual spectra were frequency corrected to correct for the small B_0 drift during the acquisition. The B_0 correction was executed for ^{1}H MR spectra by aligning the creatine peak at 3.03 ppm, and for the macromolecule spectra by aligning the macromolecule peak at 0.89 ppm, using home-written Matlab routine, as described in (5). Macromolecule spectra were then averaged between subjects for each tissue type. Residual water peak was minimized using AMARES in jMRUI (29).

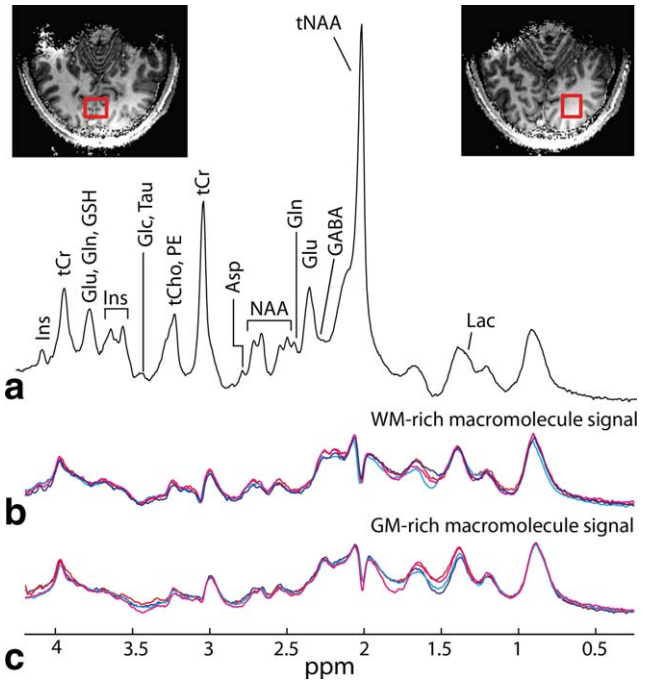

FIG. 1. ^{1}H MR spectra acquired with semi-adiabatic SPECIAL sequence (TR/TE = 7500/12 ms, vector size = 2048 pts, NT = 16 × 2) in GM-rich tissue allowing the quantification of 11 metabolites with CRLB below 20% (**a**). Macromolecule spectra (TR/TI/TE = 7500/950/12 ms, NT = 32 × 2) were acquired from 4 different subjects in occipital WM-rich (**b**) and GM-rich (**c**) VOIs. Insets: location of the voxel in the GM-rich (left) and WM-rich (right) tissue in occipital lobe. A line-broadening of 2 Hz was applied to all the spectra.

Because of the heterogeneity of the T_1 of the metabolites, some metabolite residuals remained in the measured macromolecule spectra and were identified by acquiring ^{1}H spectra using the same sequence parameters, except a long TE (TE = 30 ms). The remaining methyl groups in the GM-rich macromolecule signal consisted of N-acetylaspartate (NAA at 2.01 ppm), total choline (tCho at 3.19 ppm), and total Creatine (tCr at 3.92 ppm) (Fig. 2.1.c). On the other hand, NAA (2.01 ppm), N-acetylaspartylglutamate (NAAG at 2.2 ppm), tCho (3.19 ppm), and tCr (3.03 ppm and 3.92 ppm) residuals were detected in the WM-rich macromolecule signal (Fig. 2.2.c). Metabolite residuals were assigned to specific metabolites according to their spectral positions (30) and modeled with jMRUI (AMARES) with a set of singlet lorentzian functions, as described in Schaller et al (15). Finally, the modeled fits were subtracted from the average macromolecule spectra to provide metabolite-free macromolecule spectra. A line broadening of 2 Hz was applied to the macromolecule spectrum. To calculate the standard deviation, the sum of the macromolecule signal and the spline baseline were scaled to identical peak height at 0.9 ppm across subjects. The averaged and metabolite-free macromolecule spectrum was finally integrated to the LCModel basis set.

All spectra were fitted and quantified with LCModel (31,32) using a basis set including 20 simulated spectra

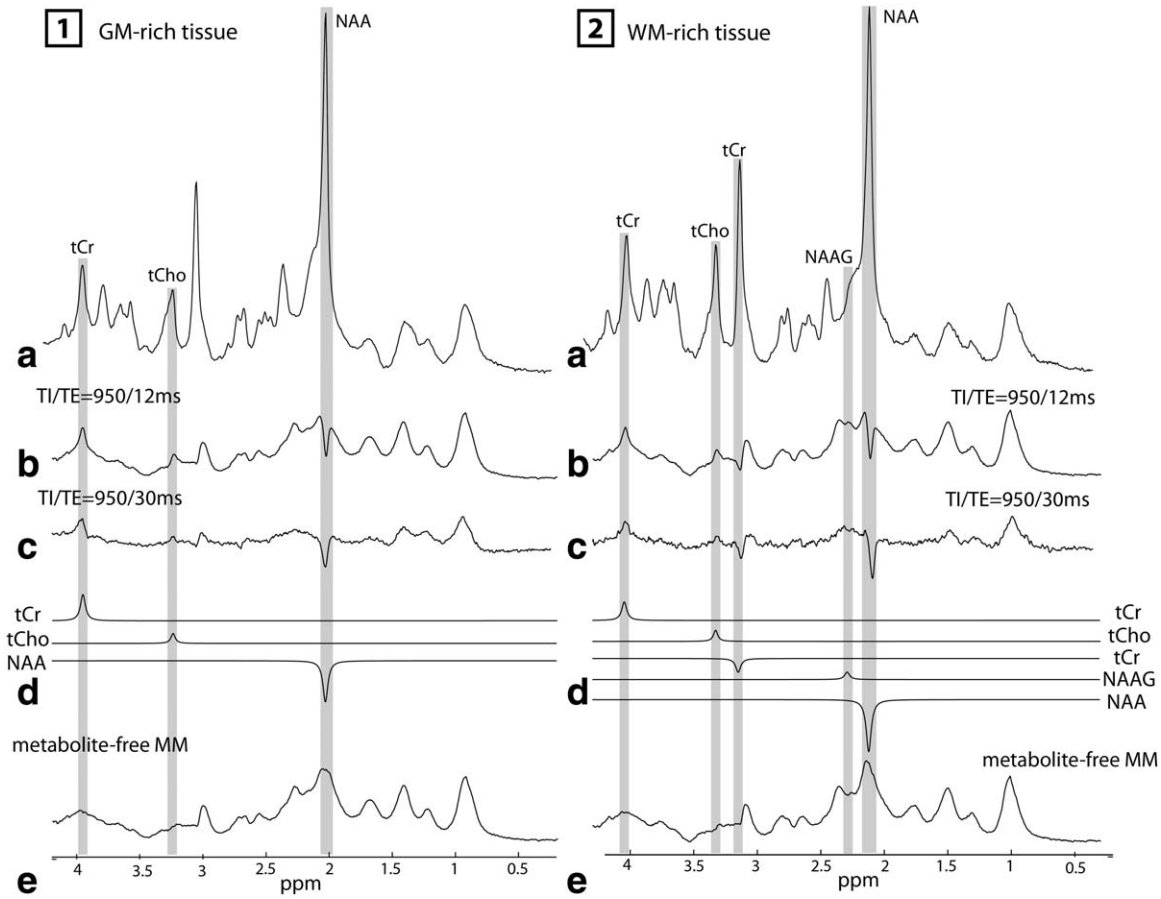

FIG. 2. Data processing of the ^{1}H MR spectra acquired in occipital WM-rich (1) and GM-rich (2) tissue. ^{1}H spectra acquired with semi-adiabatic SPECIAL sequence (**a**) and the averaged macromolecule spectrum (**b**) measured using the inversion-recovery method (n = 4). Experimentally measured macromolecule signal with the same sequence parameters, except TE = 30 ms (**c**). Residual signals were observed in the GM-rich tissue for NAA (2.01 ppm), tCho (3.19 ppm), and tCr (3.9 ppm) and in the WM-rich tissue for NAA (2.01 ppm), NAAG (2.2 ppm), tCho (3.19 ppm), and tCr (3.01 and 3.9 ppm). Metabolite residuals were fitted with jMRUI (AMARES) (**d**) and then were subtracted or added to the averaged macromolecule spectra to provide a metabolite-free macromolecule signal (**e**). A line-broadening of 2 Hz was applied to all the spectra.

of metabolites using published values for chemical shift and J-coupling constants (30,33) and an experimentally measured metabolite-free macromolecule baseline (either GM-rich or WM-rich). A concentration of total creatine of 8 μmol/g was used as an internal reference. The LCModel analysis was carried out from 0.2 ppm to 4.2 ppm. Metabolites quantified with CRLBs below 30% for at least one of the analyses were reported. The metabolite concentrations obtained using two tissue-specific basis sets were compared based on a two-way analysis of variance test with Bonferroni post-test corrections.

RESULTS

After adjustments of first- and second-order shims, the water linewidth was 12.8 ± 0.6 Hz in the GM-rich and WM-rich VOI [mean ± standard deviation (SD)]. The 6 mL VOI was placed in a region predominantly composed of WM tissue or of GM tissue (insets in Fig. 1). The mean content of the WM-rich VOI was composed of 60 ± 3% of WM tissue (mean ± SD, n = 4). Similarly, the GM-rich voxel was composed of 76 ± 4% of GM tissue (mean ± SD, n = 4). The mean SNR of N-acetylaspartate of a pair of scans acquired in GM-rich and WM-rich tissue were 57 ± 6 and 45 ± 10 (mean ± SD; n = 5).

The macromolecule spectra were acquired using a TI of 950 ms from both VOI in four subjects (Fig. 1b and c) and averaged (Fig. 2b). The remaining residual signals of metabolite methyl groups (Fig. 2c) were fitted with jMRUI (AMARES) (Fig. 2d). After removing the residual signals using jMRUI, a metabolite-free macromolecule spectrum was obtained for each VOI (Fig. 2e).

To estimate the variability of the macromolecule signal across subjects, the standard deviation of the macromolecule signal (n = 4) was calculated for each VOI. The observed standard deviation was on average 5 ± 3 a.u. from 1 to 2 ppm, 2 ± 1 a.u. from 2 to 3 ppm and 3 ± 1 a.u. from 3 to 4 ppm in GM-rich VOI (the height of the macromolecule peak at 0.9 ppm was used as an internal reference with 100 a.u.). For the same spectral regions and the same reference peak, the mean standard deviation was 4 ± 2 a.u., 2 ± 2 a.u., and 2 ± 1 a.u. in the

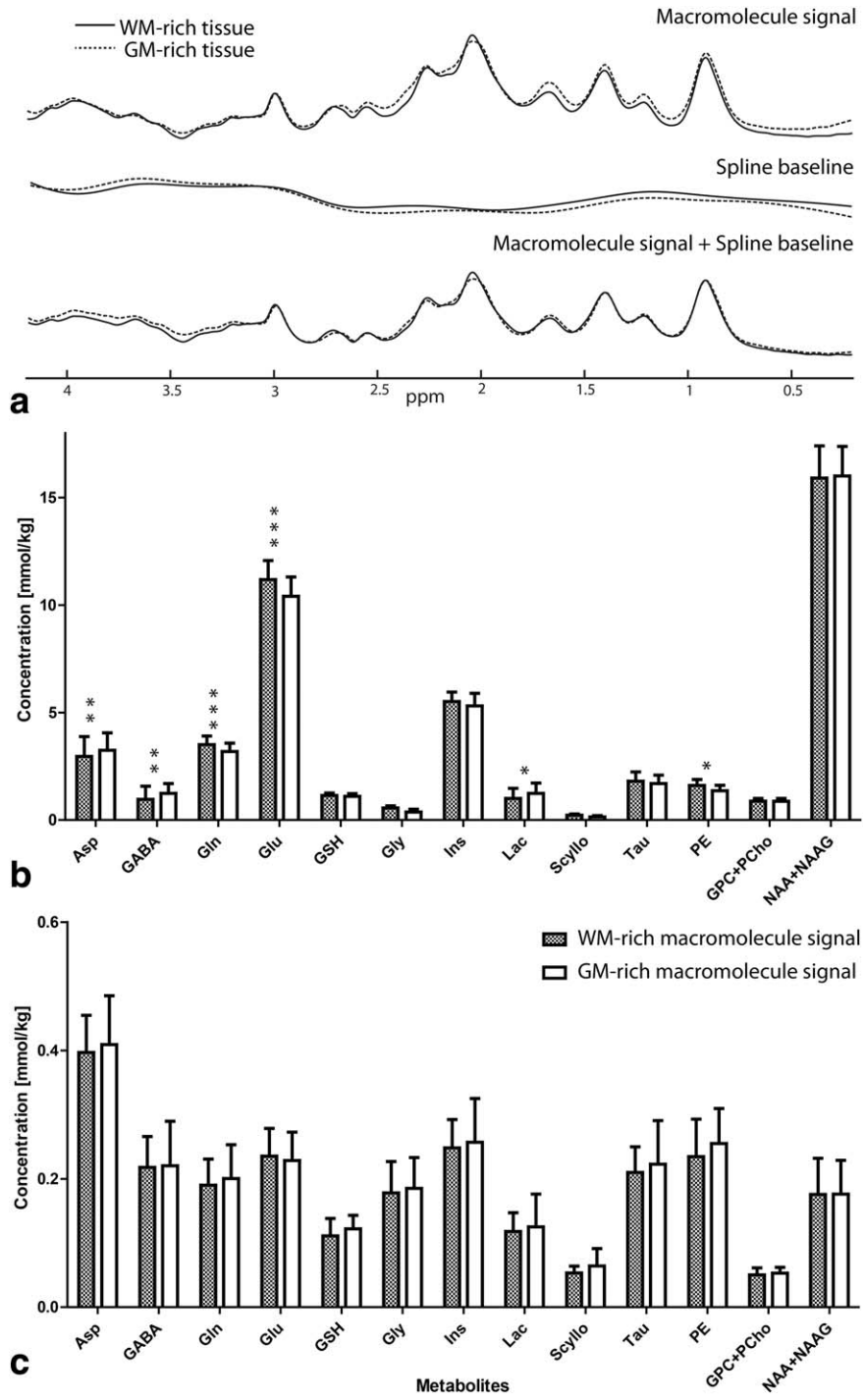

FIG. 3. ^{1}H MR spectra were acquired for ten subjects in the GM occipital lobe and were quantified with LCModel using the macromolecule signal measured in the GM-rich (broken line) or WM-rich tissue (full line). The fit macromolecule signal (**a**, top), the spline baseline (A, middle) and the sum of the macromolecule signal and the spline baseline (A, bottom) are shown. Same amplitude at 0.9 ppm was fixed for the sum of the macromolecule signal and the spline baseline. Mean metabolite concentration (**b**) and mean CRLB (**c**) were obtained using LCModel ($n = 5$). Only metabolites with mean CRLB below 30% for at least one of the approaches were reported. Data are reported in μmol/g and expressed as mean ± SD. Significant concentration changes ($^*P < 0.05$, $^{**}P < 0.01$, and $^{***}P < 0.001$) were observed for 6 metabolites. GABA, PE, and Lac were not quantified for one subject.

WM-rich VOI. The minor fluctuations of the macromolecule signal from 1.5 to 2 ppm were mainly observed because of variable suppression efficiency of the extracerebral lipid signals.

To compare the both macromolecule signals, WM-rich macromolecule signal was compared with that of acquired in GM-rich tissue. WM-rich macromolecule signal was relatively lower than the GM-rich macromolecule signal from 1.5 to 1.8 ppm and from 2.3 to 2.5 ppm with mean difference over these regions of 7% and 12% (relative to the reference peak height at 0.9 ppm), respectively. After LCModel quantification of ^{1}H MR spectra, the fitting of the macromolecule signal using the WM-rich or GM-rich experimentally measured macromolecule signal showed similar differences at 1.5–1.8 ppm and 2.3–2.5 ppm (Fig. 3a, top). Spline baselines showed comparable pattern between the two approaches with minor differences opposite to those observed for the macromolecule signals (Fig. 3a, middle). The patterns of the sum of macromolecule signal and spline baseline were strongly similar between the two approaches (Fig. 3a, bottom) with mean differences of 3% from 1.5 to 1.8

ppm, 4% from 2.3 to 2.5 ppm and 8% from 3.2 to 4.2 ppm (relative to the reference peak height at 0.9 ppm).

To determine whether the slightly different macromolecule signals affect the quantification of the neurochemical profile within experimental error, ^{1}H MR spectra acquired in the GM-rich VOI were quantified ($n = 10$) and metabolite concentrations (Fig. 3b) and CRLBs (Fig. 3c) were determined using LCModel. Two LCModel basis sets containing averaged macromolecule spectra, acquired either in predominant GM-rich or WM-rich tissue, were used for quantification. When using either basis set, ^{1}H MR spectra were well fitted judging from the flat fit residual (data not shown). The 11 metabolites Aspartate (Asp), total Creatine (tot Cr), Glutamine (Gln), Glutamate (Glu), Glutathione (GSH), myo-Inositol (Ins), Lactate (Lac), tot NAA, Taurine (Tau), phosphorylethanolamine (PE), and total Choline (GPC+PCho) were reliably quantified with a mean CRLB below 20% with both basis sets. Additionally, 1 other metabolites Scyllo-inositol (Scyllo) was reported with a mean CRLB below 30% only when using the WM macromolecule signal and γ-aminobutyric acid (GABA) only when using the GM-rich macromolecule signal. The metabolite concentration differences were below 0.3 μmol/g for all metabolites, except for Glu (± 0.8 μmol/g). The differences were significant ($P < 0.05$) for 6 metabolites (Asp, GABA, Glu, Gln, Lac and PE), but within standard deviation. CRLB differences (in μmol/g) were not significant between the two approaches ($P > 0.05$) and mean CRLBs were below 0.4 μmol/g for all metabolites (Fig. 3c).

The same analysis was also performed for WM-rich ^{1}H spectra with similar results. The same 11 metabolites were reliably quantified with a mean CRLB below 20% with both basis sets. GABA was only quantified with CRLB below 30% when using the GM-rich macromolecule signal in the basis set. All the concentration differences were below 0.3 μmol/g, except for Glu, total NAA, and GABA (± 0.5–0.7 μmol/g). The metabolite changes were significant for Asp, GABA, Glu, Ins, Tau, PE, and total NAA. The mean CRLB was below 0.3 μmol/g for all the reliably quantified metabolites.

DISCUSSION AND CONCLUSION

In this study, we measured and compared the macromolecule signal from two VOIs (GM-rich or WM-rich, Figs. 1 and 2). Relatively small differences were observed between the macromolecule signal pattern from 1.5 to 1.8 ppm and from 2.3 to 2.5 ppm. The neurochemical profiles, when using either of the two macromolecule signals, were similar for 11 reliably quantified metabolites (CRLB < 20%) with relatively small concentration differences (< 0.3 μmol/g), except Glu (± 0.8 μmol/g) (Fig. 3b).

Macromolecule signals were acquired for each subject in occipital WM-rich and GM-rich VOIs (Fig. 1b and c). Each macromolecule signal was reproducible through the entire spectral region. The macromolecule signal pattern variability over the spectral range was below 5% of the signal at 0.9 ppm. Chong et al (21) observed a relatively large variance of the macromolecule baseline between subjects and concluded that macromolecule signals were not constant between subjects. However, in our study, the localization performance of the sequence, specifically the efficiency of subcutaneous lipids suppression, and apparent reproducibility of the macromolecule pattern (Fig. 1) suggests that a reliable and stable macromolecule signal can be measured in healthy subjects at 7T.

The positive and negative residual signals of metabolite methyl groups in the averaged macromolecule signals occur at spectral positions, which corresponded to published values of metabolites chemical shift (30) and in agreement with recently published metabolites T_1 relaxation times at 7T (10). The metabolite residuals to be removed from the macromolecule signal were different between GM and WM macromolecule signal (see Methods and Fig. 2). In particular, a resonance was observed constantly for all subjects around 2.2 ppm for the WM-rich macromolecule signal and not for the GM-rich macromolecule signal (Fig. 1). According to the spectral position and to recently reported metabolite T_1 values in WM-rich and GM-rich tissues at 7T (10), the residual was attributed to NAAG. In addition, NAAG has been reported (34) to have a higher concentration in WM-rich tissue compared with GM-rich tissue. Thus, it was not considered as part of the macromolecule signal and removed using jMRUI.

To further investigate the tissue specificity of the pattern of the macromolecule resonances, the metabolite-free macromolecule spectrum acquired in WM-rich tissue was overlapped from that acquired in GM-rich tissue (Fig. 3a). At a TI of 950 ms, the macromolecule signal was recovered to 80% given the reported T_1 values at 7T (10). Minor differences were observed by visual comparison between the two macromolecule signals, notably from 1.5 to 1.8 ppm and 2.3 to 2.5 ppm. These minor differences were in agreement with previously reported differences between cerebral WM-rich and GM-rich macromolecule signal (19). Nonetheless, the pattern of the two macromolecule signals was highly similar suggesting that myelin content did not substantially affect the relative amplitude of macromolecule resonances, in agreement with previous reports (7,19). The LCModel spline baseline is used to estimate the background signal including macromolecule resonances, residual water signal and lipid signal. Therefore, the inclusion of experimentally measured macromolecule signal flattened the baseline (17). In Figure 3A (middle), both spline baselines were flat with minor differences along the spectral range. The minor differences between the sum of macromolecule signal and spline baseline (Fig. 3a, top) resulted in a small systematic overestimation or underestimation of the metabolite concentrations (see below).

To compare the differences of the neurochemical profiles obtained when using the two different macromolecule basis sets, standard deviations and CRLBs of metabolite concentration were analyzed (Fig. 3b,c). The standard deviation reflects the inter-subject variability and the measurement error, while CRLB measures the error of fitted LCModel parameters (31,35). In general, metabolite quantification was highly similar between the two LCModel analyses. Systematic and thus highly significant concentration differences were observed for Glu,

Asp, GABA, Glu, Gln, Lac, and PE, which were caused by changing the basis set. Nevertheless, metabolite concentration differences were always within the experimentally determined standard deviation. In addition, metabolite quantification still remained within the range of published concentration in occipital GM tissue when using the two different macromolecule basis sets (2,24,36,37). Finally, no significant CRLB differences were observed for all the metabolites between the two analyses suggesting similar fitting precision (Fig. 3c).

In addition, ^{1}H MR spectra acquired in WM-rich tissue were quantified using the two different macromolecule basis sets (not shown). Similar to the quantification of GM-rich ^{1}H spectra, minor differences within standard deviation were observed for metabolite concentration (below 0.7 μmol/g for all the metabolites) and for CRLB (± 6%) for the 11 reliably quantified metabolites.

To determine whether the macromolecule signal varies from subject to subject and may affect the neurochemical profile, ^{1}H MR spectra were quantified using macromolecule signal for the LCModel analysis acquired from the individual subject in the same GM-rich VOI ($n = 4$). The neurochemical profiles provided by the individual macromolecule signal and by the averaged macromolecule baseline were generally similar with mean metabolite concentration differences below 0.3 μmol/g for all the metabolites quantified with CRLB $< 30\%$. In addition, CRLBs were consistent within 5%, except for Scyllo (10%). Given the small fluctuations in the macromolecule spectral pattern caused by the variation in suppression of subcutaneous lipids, the measured individual macromolecule spectra may introduce unnecessary bias. Therefore, using an average macromolecule baseline is likely to be more reliable and robust.

We conclude that a general in vivo experimentally measured macromolecule signal is sufficient to ensure reliable metabolite quantification in occipital lobe in the healthy human brain at 7T.

ACKNOWLEDGMENTS

This work was supported by the Centre d'Imagerie Bio-Médicale (CIBM) of the UNIL, UNIGE, HUG, CHUV, EPFL, the Leenards and Jeantet Foundations and SNF. The authors declare no conflict of interest.

REFERENCES

1. Gruetter R, Weisdorf SA, Rajanayagan V, Terpstra M, Merkle H, Truwit CL, Garwood M, Nyberg SL, Ugurbil K. Resolution improvements in in vivo 1H NMR spectra with increased magnetic field strength. J Magn Reson 1998;135:260–264.
2. Mekle R, Mlynarik V, Gambarota G, Hergt M, Krueger G, Gruetter R. MR spectroscopy of the human brain with enhanced signal intensity at ultrashort echo times on a clinical platform at 3T and 7T. Magn Reson Med 2009;61:1279–1285.
3. Tkac I, Oz G, Adriany G, Ugurbil K, Gruetter R. In vivo 1H NMR spectroscopy of the human brain at high magnetic fields: metabolite quantification at 4T vs. 7T. Magn Reson Med 2009;62:868–879.
4. Tkac I, Andersen P, Adriany G, Merkle H, Ugurbil K, Gruetter R. In vivo 1H NMR spectroscopy of the human brain at 7 T. Magn Reson Med 2001;46:451–456.
5. Tkac I, Gruetter R. Methodology of H NMR spectroscopy of the human brain at very high magnetic fields. Appl Magn Reson 2005;29:139–157.
6. Bartha R, Drost DJ, Menon RS, Williamson PC. Comparison of the quantification precision of human short echo time (1)H spectroscopy at 1.5 and 4.0 Tesla. Magn Reson Med 2000;44:185–192.
7. Behar KL, Ogino T. Characterization of macromolecule resonances in the 1H NMR spectrum of rat brain. Magn Reson Med 1993;30:38–44.
8. Behar KL, Ogino T. Assignment of resonance in the 1H spectrum of rat brain by two-dimensional shift correlated and J-resolved NMR spectroscopy. Magn Reson Med 1991;17:285–303.
9. Kauppinen RA, Kokko H, Williams SR. Detection of mobile proteins by proton nuclear magnetic resonance spectroscopy in the guinea pig brain ex vivo and their partial purification. J Neurochem 1992;58:967–974.
10. Xin L, Schaller B, Mlynarik V, Lu H, Gruetter R. Proton T1 relaxation times of metabolites in human occipital white and gray matter at 7 T. Magn Reson Med 2013;69:931–936.
11. Behar KL, Rothman DL, Spencer DD, Petroff OA. Analysis of macromolecule resonances in 1H NMR spectra of human brain. Magn Reson Med 1994;32:294–302.
12. Kunz N, Cudalbu C, Mlynarik V, Huppi PS, Sizonenko SV, Gruetter R. Diffusion-weighted spectroscopy: a novel approach to determine macromolecule resonances in short-echo time 1H-MRS. Magn Reson Med 2010;64:939–946.
13. Cudalbu VM, Gruetter R. Handling macromolecule signals in the quantification of the neurochemical profile. J Alzheimers Dis 2012;31(Suppl 3):S101–S115.
14. Gottschalk M, Lamalle L, Segebarth C. Short-TE localised 1H MRS of the human brain at 3 T: quantification of the metabolite signals using two approaches to account for macromolecular signal contributions. NMR Biomed 2008;21:507–517.
15. Schaller B, Xin L, Cudalbu C, Gruetter R. Quantification of the neurochemical profile using simulated macromolecule resonances at 3 T. NMR Biomed 2013;26:593–599.
16. Cudalbu C, Mlynarik V, Xin L, Gruetter R. Quantification of in vivo short echo-time proton magnetic resonance spectra at 14.1 T using two different approaches of modelling the macromolecule spectrum. Meas Sci Technol 2009;20.
17. Pfeuffer J, Tkac I, Provencher SW, Gruetter R. Toward an in vivo neurochemical profile: quantification of 18 metabolites in short-echo-time (1)H NMR spectra of the rat brain. J Magn Reson 1999;141:104–120.
18. Mlynarik V, Cudalbu C, Xin L, Gruetter R. 1H NMR spectroscopy of rat brain in vivo at 14.1Tesla: improvements in quantification of the neurochemical profile. J Magn Reson 2008;194:163–168.
19. Hofmann L, Slotboom J, Boesch C, Kreis R. Characterization of the macromolecule baseline in localized (1)H-MR spectra of human brain. Magn Reson Med 2001;46:855–863.
20. Mader I, Seeger U, Weissert R, Klose U, Naegele T, Melms A, Grodd W. Proton MR spectroscopy with metabolite-nulling reveals elevated macromolecules in acute multiple sclerosis. Brain 2001;124(Pt 5):953–961.
21. Chong DG, Kreis R, Bolliger CS, Boesch C, Slotboom J. Two-dimensional linear-combination model fitting of magnetic resonance spectra to define the macromolecule baseline using FiTAID, a Fitting Tool for Arrays of Interrelated Datasets. MAGMA 2011;24:147–164.
22. Xin L, Mlynarik V, Lei H, Gruetter R. Influence of regional macromolecule baseline on the quantification of neurochemical profile in rat brain. In Proceedings of the 18th Annual Meeting of ISMRM, Stockholm, Sweden, 2010. Abstract 321.
23. Minati L, Aquino D, Bruzzone MG, Erbetta A. Quantitation of normal metabolite concentrations in six brain regions by in-vivoH-MR spectroscopy. J Med Phys 2010;35:154–163.
24. Emir UE, Auerbach EJ, Van De Moortele PF, Marjanska M, Ugurbil K, Terpstra M, Tkac I, Oz G. Regional neurochemical profiles in the human brain measured by (1)H MRS at 7 T using local B(1) shimming. NMR Biomed 2012;25:152–160.
25. Marques JP, Kober T, Krueger G, van der Zwaag W, Van de Moortele PF, Gruetter R. MP2RAGE, a self bias-field corrected sequence for improved segmentation and T1-mapping at high field. Neuroimage 2010;49:1271–1281.
26. Van Leemput K, Maes F, Vandermeulen D, Suetens P. Automated model-based bias field correction of MR images of the brain. IEEE Trans Med Imaging 1999;18:885–896.
27. Gruetter R. Automatic, localized in vivo adjustment of all first- and second-order shim coils. Magn Reson Med 1993;29:804–811.
28. Gruetter R, Tkac I. Field mapping without reference scan using asymmetric echo-planar techniques. Magn Reson Med 2000;43:319–323.

29. Naressi A, Couturier C, Devos JM, Janssen M, Mangeat C, de Beer R, Graveron-Demilly D. Java-based graphical user interface for the MRUI quantitation package. MAGMA 2001;12:141–152.
30. Govindaraju V, Young K, Maudsley AA. Proton NMR chemical shifts and coupling constants for brain metabolites. NMR Biomed 2000;13: 129–153.
31. Provencher SW. Automatic quantitation of localized in vivo 1H spectra with LCModel. NMR Biomed 2001;14:260–264.
32. Provencher SW. Estimation of metabolite concentrations from localized in vivo proton NMR spectra. Magn Reson Med 1993;30:672–679.
33. Xin L, Gambarota G, Mlynarik V, Gruetter R. Proton T2 relaxation time of J-coupled cerebral metabolites in rat brain at 9.4 T. NMR Biomed 2008;21:396–401.
34. Pouwels PJ, Frahm J. Differential distribution of NAA and NAAG in human brain as determined by quantitative localized proton MRS. NMR Biomed 1997;10:73–78.
35. Cavassila S, Deval S, Huegen C, van Ormondt D, Graveron-Demilly D. Cramer-Rao bounds: an evaluation tool for quantitation. NMR Biomed 2001;14:278–283.
36. Mangia S, Tkac I, Gruetter R, Van De Moortele PF, Giove F, Maraviglia B, Ugurbil K. Sensitivity of single-voxel 1H-MRS in investigating the metabolism of the activated human visual cortex at 7 T. Magn Reson Imaging 2006;24:343–348.
37. Schaller B, Xin L, Gruetter R. Influence of tissue specific macromolecule baseline on the metabolite quantification in human brain at 7 Tesla. In Proceedings of the 12th Annual Meeting of ISMRM, Melbourne, Australia, 2012. Abstract 3496.